

Article

Study of Transversely Isotropic Visco-Beam with Memory-Dependent Derivative

Kulvinder Singh ¹, Iqbal Kaur ² and Eduard-Marius Craciun ^{3,4,*}¹ CSE Department, UIET, Kurukshetra University, Kurukshetra 136118, Haryana, India; ksingh2015@kuk.ac.in² Department of Mathematics, Government College for Girls Palwal, Kurukshetra 136118, Haryana, India; bawahanda@gmail.com³ Faculty of Mechanical, Industrial and Maritime Engineering, “Ovidius” University of Constanta, 900527 Constanta, Romania⁴ Academy of Romanian Scientists, Ilfov Street, 030167 Bucharest, Romania

* Correspondence: mcraciun@univ-ovidius.ro

Abstract: Based on the modified Moore–Gibson–Thompson (MGT) model, transversely isotropic visco-thermoelastic material is investigated for frequency shift and thermoelastic damping. The Green–Naghdi (GN) III theory of thermoelasticity with two temperatures is used to express the equations that govern heat conduction in deformable bodies based on the difference between conductive and dynamic temperature acceleration. A mathematical model for a simply supported scale beam is formed in a closed form using Euler Bernoulli (EB) beam theory. We have figured out the lateral deflection, conductive temperature, frequency shift, and thermoelastic damping. To calculate the numerical values of various physical quantities, a MATLAB program has been developed. Graphical representations of the memory-dependent derivative’s influence have been made.

Keywords: transversely isotropic viscoelastic; beam; memory-dependent derivative; Moore–Gibson–Thompson model; thermoelastic damping; frequency shift

MSC: 74D99; 35D40; 35Q74

Citation: Singh, K.; Kaur, I.; Craciun, E.-M. Study of Transversely Isotropic Visco-Beam with Memory-Dependent Derivative. *Mathematics* **2023**, *11*, 4416. <https://doi.org/10.3390/math11214416>

Academic Editor: Matjaz Skrinar

Received: 3 October 2023

Revised: 17 October 2023

Accepted: 24 October 2023

Published: 25 October 2023



Copyright: © 2023 by the authors. Licensee MDPI, Basel, Switzerland. This article is an open access article distributed under the terms and conditions of the Creative Commons Attribution (CC BY) license (<https://creativecommons.org/licenses/by/4.0/>).

1. Introduction

In modern engineering structures, materials are often exposed to high temperatures, which makes viscoelastic materials, such as polymer science, of great interest. A certain amount of viscoelastic response is evident in all materials. Among the most common metals are steel, aluminium, and copper. If a material exhibits both viscous and elastic properties when deformed, it is termed viscoelastic. When linear materials show dependency on both time and temperature, they are described as rheological viscoelastic materials. As a consequence of engineering structures’ variation in temperature, approximating their material characteristics no longer holds even in an approximation context. Temperature affects the thermal and mechanical properties of materials, so it is necessary to consider the temperature dependence of their properties when performing a thermal stress analysis. Heat conductance is crucial in materials science and related sciences, especially at high working temperatures. Depending on the circumstances, metals and other materials may react differently to temperature changes. Free electrons are the main cause of conductivity in metals. As a general rule, a metal’s thermal conductivity (Kelvin) is proportional to its electric conductivity at absolute temperatures.

Visco-thermoelasticity and variational laws in irreversible thermodynamics were discussed by Biot [1]. Using an elastic moduli model and relaxations as parameters, Drozdov [2] developed a thermo-viscoelasticity constitutive model. Applied magneto-thermo-viscoelastic media were studied by Bera [3]. An isotropic visco-thermoelastic model was developed by Ezzat and El-Karamany [4] to investigate volume relaxations in

viscoelasticity. Ezzat et al. [5] developed the equation of generalized thermo-viscoelasticity with one relaxation time and two relaxation times, ignoring the volume’s relaxation effects. Visco thermoelastic micro-polar transversely isotropic (TI) media were studied by Kumar et al. [6] to determine the effect of viscosity on the amplitude ratios of plane waves. In contrast, Green and Naghdi [7–9] presented Green–Naghdi (GN) theories of thermoelasticity with and without energy dissipation. A generalized fractional-order thermoelasticity (FOT) model, introduced by Povstenko [10], introduced both classical thermoelasticity and generalized thermoelasticity with GN.

Several academic works have recently analysed and interpreted the Moore–Gibson–Thompson (MGT) equation because of its wide range of applications. There are several important applications of the MGT equation, including fluid dynamics and viscoelasticity [11]. According to Lasiecka and Wang [12], certain fluid dynamics can be modelled by a differential equation of the third order. Quintanilla [13,14] used the MGT equation with 2T to develop a new model of heat conduction. The modified Fourier equation, also known as the MGT equation, is as follows:

$$\left(1 + \tau_0 \frac{\partial}{\partial t}\right) q = -K_{ij} \nabla T - K_{ij}^* \nabla \vartheta, \text{ where, } \dot{\vartheta} = T \tag{1}$$

Later, the memory effect of thermoelasticity was subsequently demonstrated with a better model of MDD (rate of sudden change dependent on past state). “MDD is defined in an integral form of a common derivative with a kernel function on a slip-in interval”. Wang and Li [15] presented the first-order MDD with respect to time delay $\tau_0 > 0$ for a fixed time t , for the differentiable function $f(t)$:

$$D_{\tau_0} f(t) = \frac{1}{\tau_0} \int_{t-\tau_0}^t K(t-\xi) f'(\xi) d\xi, \tag{2}$$

Taylor’s series of MDD may be used to extend $q(x, t + \tau_0)$ while ignoring words up to the first order in time delay:

$$q(x, t + \tau_0) = q(x, t) + \tau_0 D_{\tau_0} q(x, t), \tag{3}$$

Thus, Fourier’s law in the theory of generalized heat conduction is provided by Ezzat et al. [16] using the Taylor series of MDD.

$$q(x, t) + \tau_0 D_{\tau_0} q(x, t) = -KT_{,i}, (0 < \tau_0 \leq 1), \tag{4}$$

The selection of the kernel functions $K(t - \xi)$ and τ_0 is influenced by the characteristics of the raw materials. Following Ezzat et al. [16–18], the $K(t - \xi)$ is used here in the form

$$K(t - \xi) = 1 - \frac{2\beta}{\tau_0}(t - \xi) + \frac{\alpha^2}{\tau_0^2}(t - \xi)^2 = \begin{cases} 1, & \alpha = 0, \beta = 0, \\ 1 + (\xi - t)/\tau_0, & \alpha = 0, \beta = 1/2, \\ \xi - t + 1, & \alpha = 0, \beta = \tau_0/2, \\ [1 + (\xi - t)/\tau_0]^2, & \alpha = 1, \beta = 1. \end{cases} \tag{5}$$

Despite this, several researchers such as Marin [19,20], Abbas and Marin [21], Kaur et al. [22,23], Van Do et al. [24], Doan et al. [25], Craciun et al. [26], Lata et al. [27], Jafari et al. [28], Craciun et al. [29], Malik et al. [30], and Sharma and Marin [31] studied the theories of thermoelasticity. Besides this, there have not been any studies on frequency shift and thermoelastic damping in visco-beams with the MGT and MDD theories of thermoelasticity.

In this research, the GN III theory of thermoelasticity and the Moore–Gibson–Thompson (MGT) equation have been revisited, and they are adopted to analyse the free vibrations in visco-thermoelastic beams with MDD. EB beam theory has been used to formulate the

mathematical simulation for the visco-beams. The effect of MDD on the various quantities is graphically depicted.

2. Basic Equations

The basic equations for an anisotropic thermo-visco-elastic medium without heat sources and body forces [8,32,33] utilizing the MGT and MDD theories are as follows:

1. The stress–displacement–temperature relation:

$$t_{ij} = \tau_m C_{ijkl} e_{kl} - \tau_m \beta_{ij} T, \tag{6}$$

where $\tau_m = 1 + \eta \frac{\partial}{\partial t}$, and η is the viscoelastic relaxation time due to the viscosity.

2. The strain–displacement relation:

$$e_{ij} = \frac{1}{2} (u_{i,j} + u_{j,i}), \quad i, j = 1, 2, 3. \tag{7}$$

3. The MGT thermoelastic heat conduction equation with MDD is

$$K_{ij} \dot{\phi}_{,ij} + K_{ij}^* \phi_{,ij} = \left(1 + \tau_0 D \tau_0 - \eta^2 \nabla^2 \right) \left(\beta_{ij} \tau_m T_0 \dot{e}_{ij} + \rho C_E \ddot{T} \right), \tag{8}$$

where

$$T = \varphi - a_{ij} \phi_{,ij}, \tag{9}$$

$$\beta_{ij} = C_{ijkl} \alpha_{ij}, \tag{10}$$

$\beta_{ij} = \beta_i \delta_{ij}$, $K_{ij} = K_i \delta_{ij}$, $K_{ij}^* = K_i^* \delta_{ij}$, i is not summed. C_{ijkl} are elastic parameters and have symmetry ($C_{ijkl} = C_{klij} = C_{jikl} = C_{ijlk}$).

3. Mathematical Modelling of the Problem

As illustrated in Figure 1, we have taken a visco-beam with length ($0 \leq x \leq L$), width ($-\frac{b}{2} \leq y \leq \frac{b}{2}$), and thickness ($-\frac{h}{2} \leq z \leq \frac{h}{2}$) in Cartesian coordinates. Let the beam’s x -axis serve as its axis. Its two endpoints should be at $x = 0$ and $x = h$, and the origin should be located in the middle of the end at $x = 0$. Consider that beam is free from any stress and strain and is at a uniform temperature T_0 in a stable position. Additionally, the upper and bottom surfaces of the beam do not experience any heat transfer; therefore,

$$\frac{\partial \varphi}{\partial z} = 0, \quad \text{at } z = \pm \frac{h}{2}. \tag{11}$$

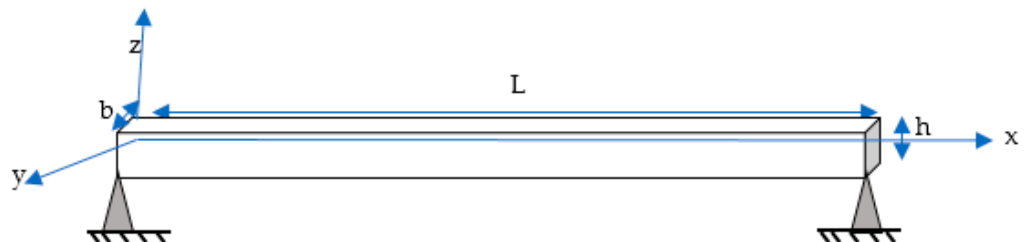


Figure 1. Diagram of the visco-beam.

The EB model describes that “any plane cross-section, initially perpendicular to the axis of the beam remains plane and perpendicular to the neutral surface during bending”.

Therefore, according to Youssef et al. [34], the following displacement components are given for small deflection:

$$u(x, y, z, t) = -z \frac{\partial w}{\partial x}, \quad v(x, y, z, t) = 0, \quad w(x, y, z, t) = w(x, t), \tag{12}$$

The 1D constitutive Equation (6) using Equation (12) becomes

$$t_{xx} = -C_{11} \tau_m z \frac{\partial^2 w}{\partial x^2} - \beta_1 \tau_m T, \tag{13}$$

where $\beta_1 = (C_{11} + C_{13})\alpha_1 + C_{13}\alpha_3$.

The thermoelastic parameter $\beta_3 = 2C_{13}\alpha_1 + C_{33}\alpha_3$ does not exist along the z-axis according to the EB hypothesis.

The flexural moment of the cross-section $M(x, t)$ for the beam is provided by Rao [35] as

$$M(x, t) = - \int_{-\frac{h}{2}}^{\frac{h}{2}} \int_{-\frac{b}{2}}^{\frac{b}{2}} t_{xx} z dz dy = C_{11} \tau_m I \frac{\partial^2 w}{\partial x^2} + \beta_1 \tau_m M_T, \tag{14}$$

where

$$M_T = b \int_{-\frac{h}{2}}^{\frac{h}{2}} T z dz, \tag{15}$$

$$I = \frac{bh^3}{12}.$$

Since $T \equiv T(x, z, t)$ and $\varphi \equiv \varphi(x, z, t)$, the thermodynamic temperature of a transversely isotropic beam from Equation (14) is given by

$$T = \left\{ \varphi - \left(a_1 \frac{\partial^2 \varphi}{\partial x^2} + a_3 \frac{\partial^2 \varphi}{\partial z^2} \right) \right\}. \tag{16}$$

The equation for the motion of the visco-beam without pressures in the transverse direction [35,36] is written as

$$\frac{\partial^2 M}{\partial x^2} + \rho A \frac{\partial^2 w}{\partial t^2} = 0, \tag{17}$$

where $A = bh$.

Using Equation (14) in Equation (17), we obtain

$$C_{11} I \tau_m \frac{\partial^4 w}{\partial x^4} + \beta_1 \tau_m \frac{\partial^2 M_T}{\partial x^2} + \rho A \frac{\partial^2 w}{\partial t^2} = 0. \tag{18}$$

Equation (8), with the help of Equation (12), becomes

$$\left(K_1^* + K_1 \frac{\partial}{\partial t} \right) \frac{\partial^2 \varphi}{\partial x^2} + \left(K_3^* + K_3 \frac{\partial}{\partial t} \right) \frac{\partial^2 \varphi}{\partial z^2} = -z \beta_1 T_0 (1 + \tau_0 D_{\tau_0}) \tau_m \frac{\partial^4 w}{\partial x^2 \partial t^2} + \rho C_E (1 + \tau_0 D_{\tau_0}) \frac{\partial^2}{\partial t^2} \left\{ \varphi - \left(a_1 \frac{\partial^2 \varphi}{\partial x^2} + a_3 \frac{\partial^2 \varphi}{\partial z^2} \right) \right\}. \tag{19}$$

The beam's time harmonic behaviour may be described as

$$[w(x, t), \varphi(x, z, t)] = [w(x), \varphi(x, z)] e^{i\omega t}. \tag{20}$$

The dimensionless quantities are given as

$$x' = \frac{x}{L}, \quad z' = \frac{z}{L}, \quad w' = \frac{w}{L}, \quad h' = \frac{h}{L}, \quad b' = \frac{b}{L}, \quad t' = \frac{c_1}{L} t, \quad \eta' = \frac{c_1}{L} \eta, \quad T' = \frac{T}{T_0}, \tag{21}$$

$$\varphi' = \frac{\varphi}{T_0}, \quad \rho c_1^2 = C_{11}, \quad t'_{xx} = \frac{t_{xx}}{\beta_1 T_0}, \quad a'_1 = \frac{a_1}{L^2}, \quad a'_3 = \frac{a_3}{L^2}, \quad M'_T = \frac{M_T}{T_0 L^3}.$$

Equation (21) is applied to Equations (18) and (19) to yield the non-dimensional version of these equations after suppressing the primes, which is represented as

$$I\tau_m^* \frac{\partial^4 w}{\partial x^4} + \tau_m^* \frac{\beta_1 T_0 L^4}{c_{11}} \frac{\partial^2 M_T}{\partial x^2} - AL^2 \omega^2 w = 0, \tag{22}$$

$$(K_1^* + K_1 \frac{c_1}{L} i\omega) \frac{\partial^2 \varphi}{\partial x^2} + (K_3^* + K_3 \frac{c_1}{L} i\omega) \frac{\partial^2 \varphi}{\partial z^2} = zc_1^2 \beta_1 \omega^2 (1 + \tau_0 G) \tau_m^* \frac{\partial^2 w}{\partial x^2} - \rho C_E c_1^2 \omega^2 (1 + \tau_0 G) \left\{ \varphi - \left(a_1 \frac{\partial^2 \varphi}{\partial x^2} + a_3 \frac{\partial^2 \varphi}{\partial z^2} \right) \right\}. \tag{23}$$

where $\tau_m^* = 1 + \eta i\omega$

$$G = \frac{i}{\omega} \left\{ \frac{(1 - e^{i\omega\tau_0})i}{\omega\tau_0} - 2\beta \left[\frac{(1 - i\omega\tau_0)e^{i\omega\tau_0} - 1}{(\omega\tau_0)^2} \right] + \alpha^2 \left[\frac{(i((\omega\tau_0)^2 - 2) - 2\tau\omega)e^{i\omega\tau_0} - 2i}{(\omega\tau_0)^3} \right] \right\}$$

4. Boundary Conditions

Let us assume that the beam is initially at rest and intact. As a result,

$$w(x, 0) = \frac{\partial w(x, 0)}{\partial t} = 0, \tag{24}$$

$$\varphi(x, z, 0) = \frac{\partial \varphi(x, z, 0)}{\partial t} = 0, \tag{25}$$

As considered, the ends of the beam are simply supported; therefore,

$$w(0, t) = w(L, t) = 0, \tag{26}$$

$$\frac{\partial^2 w(0, t)}{\partial x^2} = \frac{\partial^2 w(L, t)}{\partial x^2} = 0. \tag{27}$$

Now imagine that there is no heat transfer between the two surfaces of the beam, i.e., along the bottom surface $z = \frac{h}{2}$ and the upper surface $z = -\frac{h}{2}$, which results in

$$\frac{\partial \varphi}{\partial z} \left(x, \frac{h}{2}, 0 \right) = \frac{\partial \varphi}{\partial z} \left(x, -\frac{h}{2}, 0 \right) = 0. \tag{28}$$

5. Solution of the Problem along the Thickness Direction

Lifshitz and Roukes [37] state that the thermal gradient is zero in the y-direction. Additionally, “due to geometry, the thermal gradients in the plane of the cross-section along the thickness direction i.e., z-axis are much larger than those along its axis i.e., x-axis of the -beam” (i.e., $\frac{\partial^2 \varphi}{\partial x^2} \ll \frac{\partial^2 \varphi}{\partial z^2}$, hence $\frac{\partial^2 \varphi}{\partial x^2}$ can be ignored in Equation (22)), and hence Equation (22) for heat conduction may be changed to

$$\frac{\partial^2 \varphi}{\partial z^2} + \zeta_1^2 \varphi = \frac{\beta_1 \zeta_1^2 \tau_m^*}{\rho C_E} \frac{\partial^2 w}{\partial x^2}, \tag{29}$$

where

$$\zeta_1 = \sqrt{\frac{\rho C_E c_1^2 \omega^2 (1 + \tau_0 G)}{(K_3^* + K_3 \frac{c_1}{L} i\omega - a_3 \rho C_E c_1^2 \omega^2 (1 + \tau_0 G))}}.$$

Equation (29) yields the following solution:

$$\varphi(x, z) = \frac{\beta_1 \tau_m^*}{\rho C_E} \left(z - \frac{\sin \zeta_1 z}{\zeta_1 \cos \frac{\zeta_1 h}{2}} \right) \frac{\partial^2 w}{\partial x^2}. \tag{30}$$

Using Equation (30) in Equation (15) with the aid of Equation (16), we obtain

$$M_T = \frac{I\beta_1\tau_m^*}{\rho C_E} \left(1 + (-1 + a_3\zeta_1^2)f(\omega) \right) \frac{\partial^2 w}{\partial x^2}. \tag{31}$$

and using Equation (31) in Equation (22), we obtain

$$L_\omega \frac{\partial^4 w}{\partial x^4} - \omega^2 w = 0, \tag{32}$$

where

$$L_\omega = \frac{I}{AL^2} \tau_m^* [1 + \varepsilon_T (1 - (1 + a_3\zeta_1^2)f(\omega))],$$

$$\varepsilon_T = \frac{\beta_1^2 T_0 L^4}{\rho C_E},$$

$$f(\omega) = \frac{24}{\zeta_1^3 h^3} \left(\frac{\zeta_1 h}{2} - \tan \frac{\zeta_1 h}{2} \right).$$

Now, Equation (32) can also be written as

$$\frac{\partial^4 w}{\partial x^4} - \zeta^4 w = 0, \tag{33}$$

where

$$\zeta^4 = \frac{\omega^2}{L_\omega}.$$

Applying Laplace transforms defined by

$$\bar{w}(s) = \int_0^\infty w(x)e^{-sx} dx, \tag{34}$$

on Equation (33) and using boundary conditions defined by Equations (26) and (27), we obtain the following solution of Equation (33):

$$\bar{w}(s) = \frac{A_1}{2\zeta} \left(\frac{1}{s^2 + \zeta^2} + \frac{1}{s^2 - \zeta^2} \right) + \frac{A_2}{2\zeta^2} \left(\frac{1}{s^2 - \zeta^2} - \frac{1}{s^2 + \zeta^2} \right). \tag{35}$$

Now, taking the inverse Laplace transform of Equation (35) gives

$$w(x) = \frac{A_1}{2\zeta} (\sin(\zeta x) + \sinh(\zeta x)) + \frac{A_2}{2\zeta^2} (\sinh(\zeta x) - \sin(\zeta x)). \tag{36}$$

After including the dimensionless quantities defined by Equation (21) in the boundary conditions (26) and (27), solving Equation (36) at $x = L$ provides

$$\sin(\zeta)\sinh(\zeta) = 0. \tag{37}$$

which yields $\zeta_n = n\pi, n \geq 1$. Thus, the solutions for the lateral deflection from Equation (24) and the thermal moment expressions from Equation (35) for $\zeta_n = n\pi, n \geq 1$ are derived by using (31) as follows:

$$w(x, t) = \frac{1}{2} \sum_n \frac{A_n}{\zeta_n (\sin \zeta_n + \sinh \zeta_n)} \{ (\sin \zeta_n + \sinh \zeta_n) (\sin \zeta_n x + \sinh \zeta_n x) - (-\sin \zeta_n + \sinh \zeta_n) (-\sin \zeta_n x + \sinh \zeta_n x) \} e^{i\omega_n t}, \tag{38}$$

$$M_T(x, z, t) = \frac{I\beta_1\tau_m^*}{\rho C_E} \left(1 + (1 + a_3\zeta_1^2)f(\omega) \right) \sum_n \frac{A_n \zeta_n}{(\sin \zeta_n + \sinh \zeta_n)} \{ (\sin \zeta_n + \sinh \zeta_n) (-\sin \zeta_n x + \sinh \zeta_n x) - (-\sin \zeta_n + \sinh \zeta_n) (\sin \zeta_n x + \sinh \zeta_n x) \} e^{i\omega_n t}. \tag{39}$$

From Equation (32), the beam’s vibrational frequency is determined by

$$\omega_n = n^2 \pi^2 \sqrt{L\omega} = \omega_0 \sqrt{1 + \epsilon_T (1 + (1 + a_3 \zeta_1^2)) f(\omega)}, \tag{40}$$

where

$$\omega_0 = \frac{hn^2 \pi^2}{L\sqrt{12}}$$

If we replace ω with ω_0 and $f(\omega)$ with (ω_0) , we obtain the solution for all the media having $\epsilon_T \ll 1$ as follows:

$$\omega^m = \omega_0 \sqrt{1 + \epsilon_T (1 + (1 + a_3 \zeta_1^2)) f(\omega)}. \tag{41}$$

The thermoelastic damping (TED) quality, also known as the thermal quality Q-factor, may be determined by

$$Q^{-1} = 2 \left| \frac{\omega_I^n}{\omega_R^n} \right|, \tag{42}$$

where n is the mode number and is related to the transcendental roots in Equation (37), and ω_R^n and ω_I^n are the real and the imaginary parts of frequency ω^n . Due to thermal variations, the frequency shift (FS) may be given by

$$\omega_S = \left| \frac{\omega_R^n - \omega_0}{\omega_0} \right|. \tag{43}$$

6. Particular Cases

1. We can obtain the solution of physical quantities for simply supported visco-beams with the GN-II theory of thermoelasticity if $K_1 = K_3 = 0$ in Equations (38)–(43).
2. We can obtain the solution of physical quantities for simply supported visco-beams with the classical theory of thermoelasticity if we take $K_1^* = K_3^* = 0$ in Equations (38)–(43).
3. We can obtain the solution of physical quantities for simply supported cubic crystal thermoelastic visco-beams with the GN type-III theory of thermoelasticity if we take $C_{11} = C_{22} = C_{33}, C_{12} = C_{13}, C_{44} = C_{66}, \alpha_1 = \alpha_3 = \alpha', \beta_1 = \beta_3 = \beta', K_1 = K_3 = K, K_1^* = K_3^* = K^*$ in Equations (38)–(43).
4. We can obtain the solution of physical quantities for free vibrations in simply supported visco-beams with energy dissipation similar to Abbas [38] if we take $C_{11} = C_{33} = \lambda + 2\mu, C_{12} = C_{13} = \lambda, C_{44} = 2\mu, \alpha_1 = \alpha_3 = \alpha', a_1 = a_3 = a, K_1 = K_3 = K, K_1^* = K_3^* = K^*$ in Equations (38)–(43).

7. Results and Discussion

Physical information for cobalt material (transversely isotropic) for the beam was selected from Dhaliwal and Singh [39] to illustrate the theoretical results:

$$C_{11} = 3.071 \times 10^{11} \text{Nm}^{-2}, C_{12} = 1.650 \times 10^{11} \text{Nm}^{-2}, C_{13} = 1.027 \times 10^{10} \text{Nm}^{-2},$$

$$C_{33} = 3.581 \times 10^{11} \text{Nm}^{-2}, C_{44} = 1.510 \times 10^{11} \text{Nm}^{-2}, C_E = 4.27 \times 10^2 \text{Jkg}^{-1} \text{K}^{-1},$$

$$\beta_1 = 7.04 \times 10^6 \text{Nm}^{-2} \text{K}^{-1}, \rho = 8.836 \times 10^3 \text{kgm}^{-3}, T_0 = 298 \text{K},$$

$$\beta_3 = 6.90 \times 10^6 \text{Nm}^{-2} \text{K}^{-1}, L = 1 \text{m}, b = 0.01 \text{m}$$

$$K_1 = 0.690 \times 10^2 \text{Wm}^{-1} \text{K}^{-1}, K_3 = 0.690 \times 10^2 \text{Wm}^{-1} \text{K}^{-1},$$

$$K_1^* = 0.02 \times 10^2 \text{ NSec}^{-2}\text{K}^{-1}, K_3^* = 0.04 \times 10^2 \text{ NSec}^{-2}\text{K}^{-1},$$

$$\eta = 0.01, \tau_0 = 0.02. \text{ Here, we have taken } A_n = 1.$$

The following physical data for copper, which is an isotropic material, were taken:

$$\lambda = 7.76 \times 10^{10} \text{ Nm}^{-2}, \mu = 3.86 \times 10^{10} \text{ Nm}^{-2}, \rho = 8.954 \times 10^3 \text{ Kgm}^{-3},$$

$$K = 386 \text{ Wm}^{-1}\text{K}^{-1}, \alpha' = 1.78 \times 10^{-5} \text{ K}^{-1}, C_E = 383.1 \text{ JKg}^{-1}\text{K}^{-1}, T_0 = 293 \text{ K},$$

$$K^* = 1.0 \times 10^{10} \text{ Nm}^{-2}$$

A program was developed in MATLAB to determine the numerical values of w , conductive temperature φ , M_T , Q^{-1} , and ω_S , and graphs drawn for different modes of kernel function of MDD are presented in Figures 2–6.

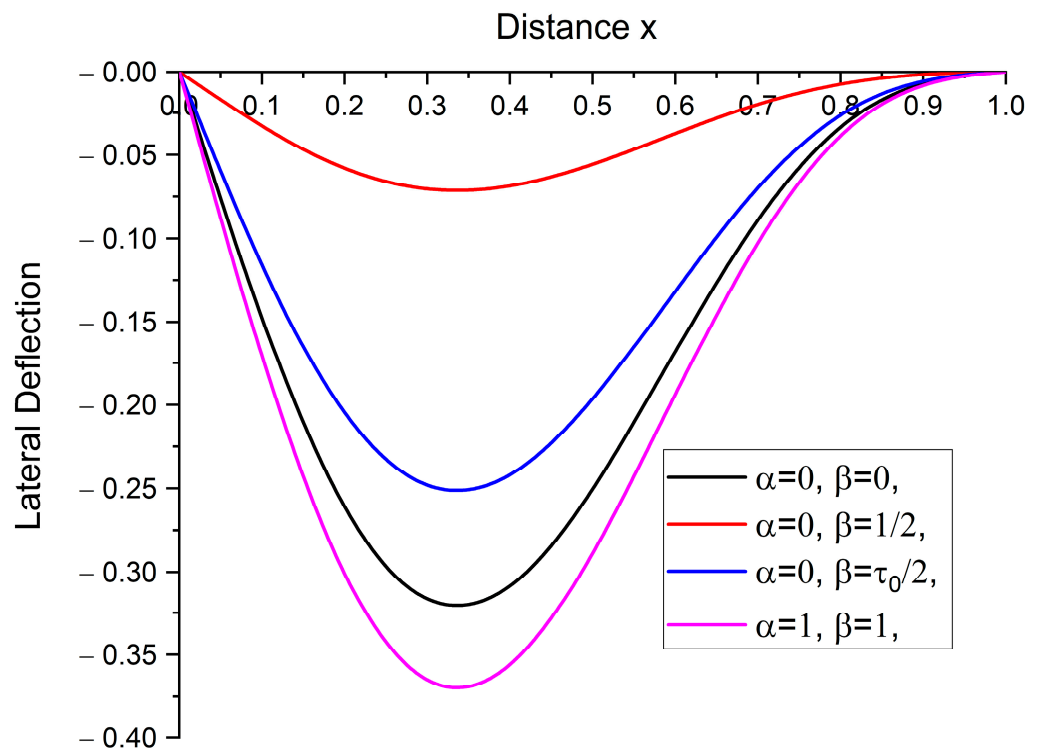


Figure 2. Graph of the lateral deflection w with respect to length of beam with different kernel function of MDD.

Figure 2 demonstrates the variation in the lateral deflection w with respect to the length of the visco-beam for different modes of kernel function $1 - \frac{2\beta}{\tau_0}(t - \xi) + \frac{\alpha^2}{\tau_0^2}(t - \xi)^2$ of MDD based on the values of α and β . As both ends of the visco-beam are simply supported, from the graph, it can be observed that the lateral deflection at $x = 0$ and $x = L$ is zero, which satisfies the boundary conditions. Moreover, for the kernel function $1 + (\xi - t)/\tau_0$ of MDD, the visco-beam shows the minimum variation as compared to when the value of the kernel function is $[1 + (\xi - t)/\tau_0]^2$. Therefore, the memory effect is clearly noticeable from the graph.

Figure 3 shows the variation in thermal moment M_T with the length of the beam for different modes of kernel function $1 - \frac{2\beta}{\tau_0}(t - \xi) + \frac{\alpha^2}{\tau_0^2}(t - \xi)^2$ of MDD based on the

values of α and β . As both ends of the visco-beam are simply supported, from the graph, it can be observed that the thermal moment at $x = 0$ and $x = L$ is zero, which satisfies the boundary conditions. Moreover, for the kernel function 1 for $\alpha = 0$ and $\beta = 0$ of MDD, the visco-beam shows the minimum variation, whereas the thermal moment is at its maximum when the value of kernel function is $[1 + (\xi - t)/\tau_0]^2$. Therefore, the memory effect is clearly noticeable from the graph.

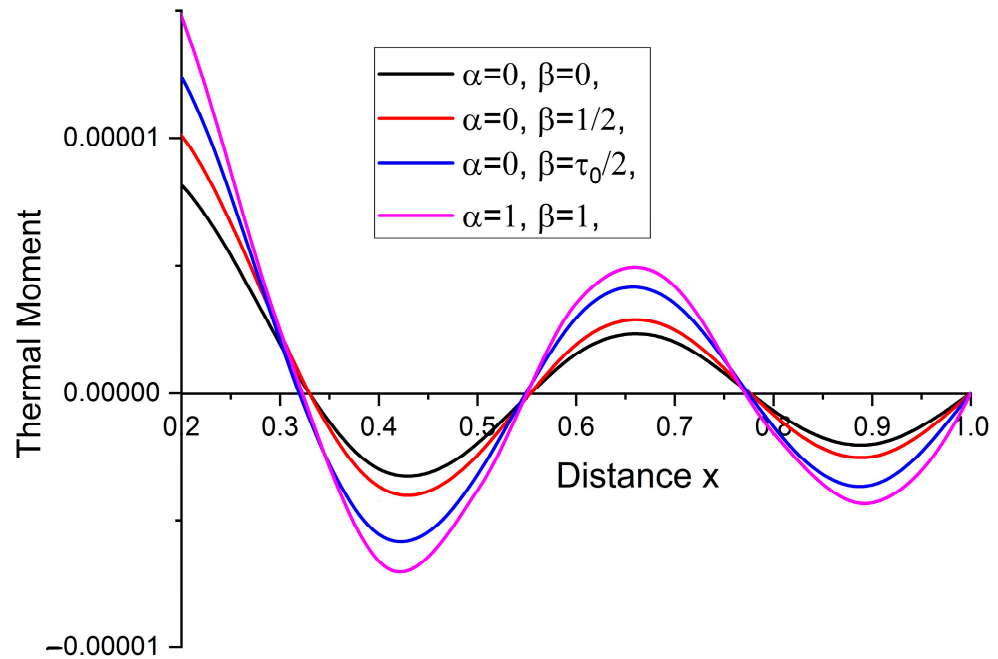


Figure 3. Graph of the thermal moment M_T with length of the beam with different kernel function of MDD.

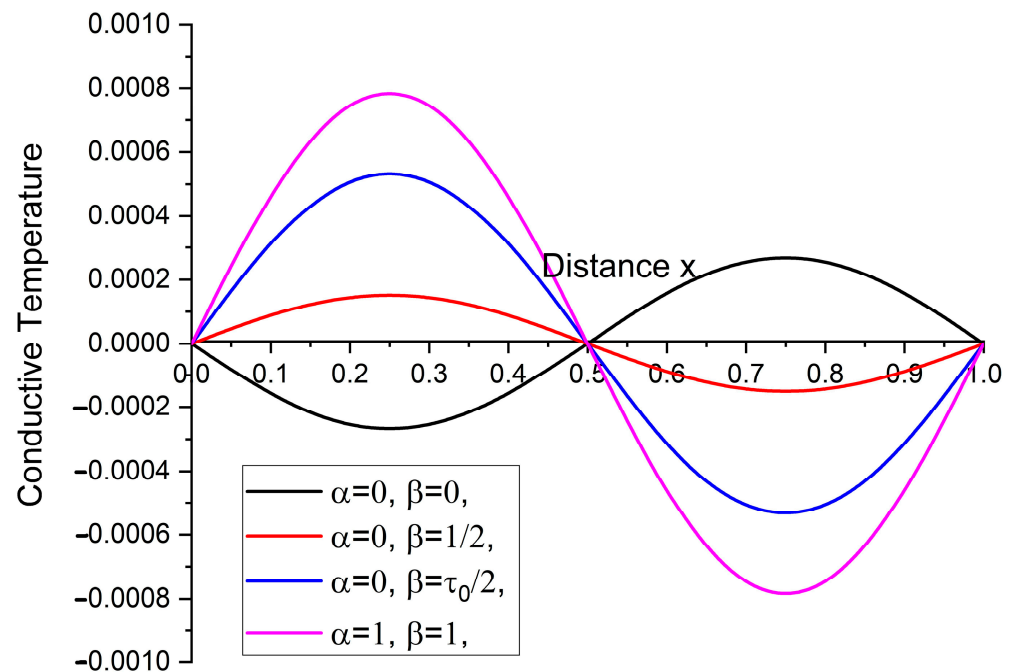


Figure 4. The conductive temperature with length x of beam with different kernel function of MDD.

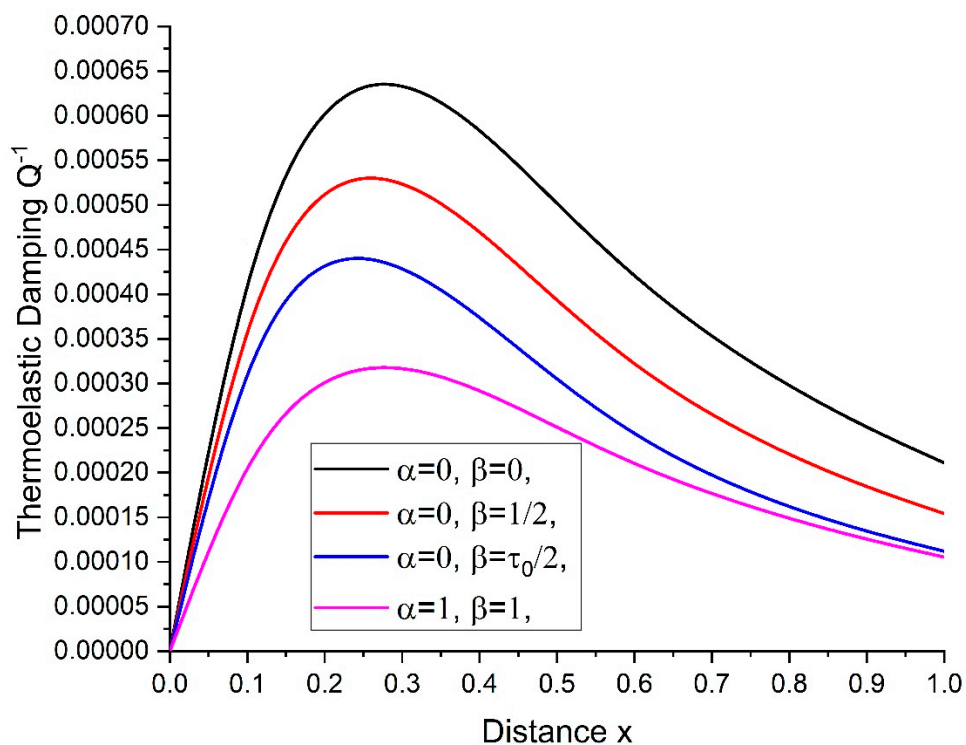


Figure 5. The thermoelastic damping Q^{-1} with length x of beam with different kernel function of MDD.

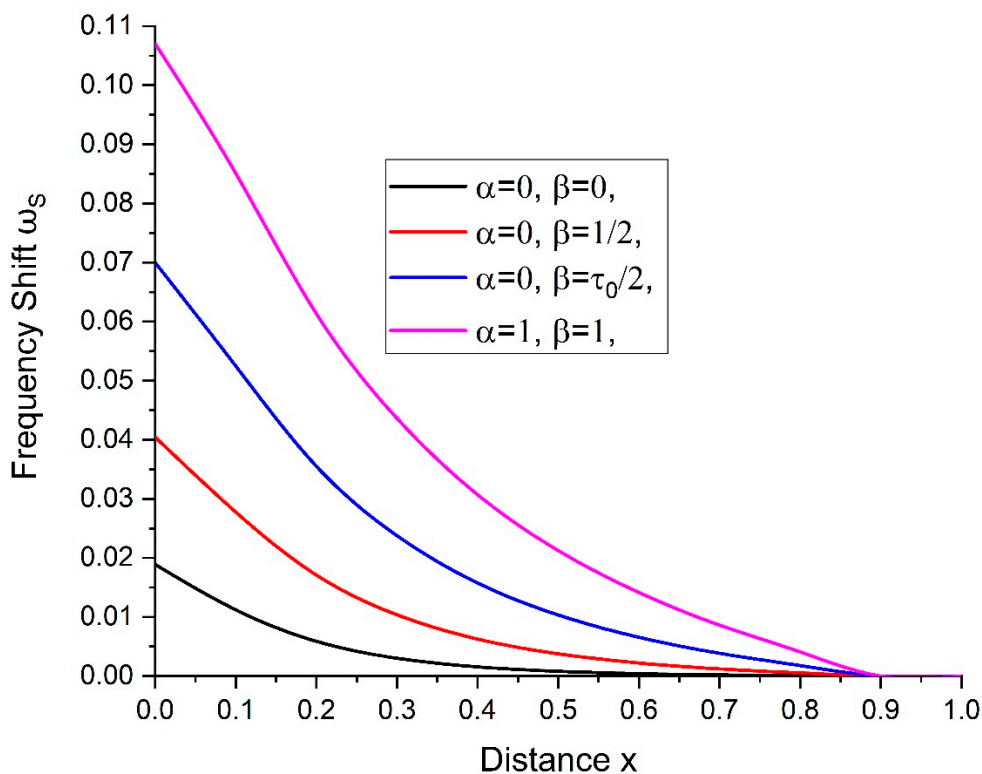


Figure 6. Graph of the frequency shift ω_s with length L of the beam with different kernel function of MDD.

Figure 4 demonstrates the variations in the conductive temperature φ with the length x for different modes of kernel function $1 - \frac{2\beta}{\tau_0}(t - \zeta) + \frac{\alpha^2}{\tau_0^2}(t - \zeta)^2$ of MDD based on the values of α and β . As both ends of the visco-beam are simply supported, from the graph, it

can be observed that the conductive temperature at $x = 0$ and $x = L$ is zero, which satisfies the boundary conditions. Moreover, for the kernel function 1 for $\alpha = 0$ and $\beta = 0$ of MDD, the visco-beam shows the minimum variation in conductive temperature and shows the opposite behaviour to other values of kernel function of MDD, whereas the conductive temperature is at its maximum when the value of kernel function is $[1 + (\zeta - t)/\tau_0]^2$. Therefore, the memory effect is clearly noticeable from the graph.

Figure 5 demonstrates the variations in the thermoelastic damping Q^{-1} with the length x for different modes of kernel function $1 - \frac{2\beta}{\tau_0}(t - \zeta) + \frac{\alpha^2}{\tau_0^2}(t - \zeta)^2$ of MDD based on the values of α and β . For the kernel function 1 for $\alpha = 0$ and $\beta = 0$ of MDD, the visco-beam shows the maximum variation in thermoelastic damping, whereas thermoelastic damping is at its minimum when the value of kernel function is $[1 + (\zeta - t)/\tau_0]^2$. Therefore, the memory effect is clearly noticeable from the graph.

Figure 6 exhibits the frequency shift ω_S with length x for different modes of kernel function $1 - \frac{2\beta}{\tau_0}(t - \zeta) + \frac{\alpha^2}{\tau_0^2}(t - \zeta)^2$ of MDD based on the values of α and β . For the kernel function 1 for $\alpha = 0$ and $\beta = 0$ of MDD, the visco-beam shows the minimum variation in thermoelastic damping, whereas the thermoelastic damping is at its maximum when the value of kernel function is $[1 + (\zeta - t)/\tau_0]^2$. Therefore, the memory effect is clearly noticeable from the graph. It is observed that as the length of the beam increases, the frequency shift ω_S abruptly decreases from its highest value to zero.

8. Conclusions

A mathematical model for a simply supported scale beam was formed in a closed form using Euler Bernoulli (EB) beam theory based on the modified Moore–Gibson–Thompson (MGT) model to investigate the frequency shift, thermoelastic damping, and other parameters of visco-beams. The Green–Naghdi (GN) III theory of thermoelasticity with two temperature- and memory-dependent derivatives was used to express the equations that govern heat conduction in deformable bodies. The solutions of PDE were obtained using Laplace transforms.

We came to the following conclusions after the discussion:

- The kernel function of the memory-dependent derivative plays a dominant role. As the kernel function changes, the amplitudes of the lateral deflection and thermal moment increase, but amplitude of the thermoelastic damping factor decreases with change in the kernel function.
- It was noticed that the frequency of time harmonic sources has a significant impact on the various properties of the beam.
- It was observed that the thermoelastic damping Q^{-1} grows first to reach the maximum values before decreasing with length. For the kernel function 1 for $\alpha = 0$ and $\beta = 0$ of MDD, the visco-beam shows the maximum variation in thermoelastic damping, whereas the thermoelastic damping is at its minimum when the value of kernel function is $[1 + (\zeta - t)/\tau_0]^2$. Therefore, the memory effect is clearly noticeable from the graph.
- As the length of the beam increases, the frequency shift ω_S decreases from its high value at the beginning to zero.
- Theoretical research and computational results demonstrate that memory effects can amplify the thermoelastic field variations.
- Theoretical research and applications in viscoelastic materials have become crucial for solid mechanics because of the quick development of polymer science and the plastics industry, as well as the widespread use of materials that can withstand high temperatures in contemporary technology, sensing and actuation, mechanical resonators, and the integration of biology and geology into engineering.

Author Contributions: K.S.: conceptualization, effective literature review, experiments and simulation, investigation, methodology, software, supervision, validation, visualization, writing—original draft. I.K.: idea formulation, conceptualization, formulated strategies for mathematical modelling, methodology refinement, formal analysis, validation, writing—review and editing. E.-M.C.: conceptualization, effective literature review, formulated strategies for mathematical modelling, investigation, methodology, supervision, validation, visualization, writing—review and editing. All authors have read and agreed to the published version of the manuscript.

Funding: No fund/grant/scholarship has been taken for this research work.

Data Availability Statement: For the numerical results, silicon material was taken from Mahdy et al. [40].

Conflicts of Interest: The authors declare that they have no conflict of interest.

Nomenclature

δ_{ij}	Kronecker delta
C_{ijkl}	Elastic parameters
β_{ij}	Thermal elastic coupling tensor
T	Absolute temperature
T_0	Reference temperature
φ	Conductive temperature
t_{ij}	Stress tensors
e_{ij}	Strain tensors
u_i	Components of displacement
ρ	Medium density
C_E	Specific heat
a_{ij}	Two temperature parameters
ω	Frequency
I	Moment of inertia
$C_{11}I$	Flexural rigidity of the visco-beam
s	Laplace transform parameter
ε_T	Thermoelastic coupling
A	Area of cross-section
M_T	Thermal moment
$M(x, t)$	Flexural moment
$w(x, t)$	Lateral deflection
t	Time
α_{ij}	Linear thermal expansion coefficient
K_{ij}	Thermal conductivity
K_{ij}^*	Materialistic constant

References

1. Biot, M.A. Theory of Stress-Strain Relations in Anisotropic Viscoelasticity and Relaxation Phenomena. *J. Appl. Phys.* **1954**, *25*, 1385–1391. [[CrossRef](#)]
2. Drozdov, A.D. A Constitutive Model in Thermoviscoelasticity. *Mech. Res. Commun.* **1996**, *23*, 543–548. [[CrossRef](#)]
3. Bera, R.K. Propagation of Waves in Random Rotating Infinite Magneto-Thermo-Visco-Elastic Medium. *Comput. Math. Appl.* **1998**, *36*, 85–102. [[CrossRef](#)]
4. Ezzat, M.A.; El-Karamany, A.S. The Relaxation Effects of the Volume Properties of Viscoelastic Material in Generalized Thermoelasticity. *Int. J. Eng. Sci.* **2003**, *41*, 2281–2298. [[CrossRef](#)]
5. Ezzat, M.A. State Space Approach to Generalized Magneto-Thermoelasticity with Two Relaxation Times in a Medium of Perfect Conductivity. *Int. J. Eng. Sci.* **1997**, *35*, 741–752. [[CrossRef](#)]
6. Kumar, R.; Sharma, K.D.; Garg, S.K. Reflection of Plane Waves in Transversely Isotropic Micropolar Viscothermoelastic Solid. *Mater. Phys. Mech.* **2014**, *22*, 1–14.
7. Green, A.E.; Naghdi, P.M. A Re-Examination of the Basic Postulates of Thermomechanics. *Proc. R. Soc. Lond. Ser. A Math. Phys. Sci.* **1991**, *432*, 171–194. [[CrossRef](#)]
8. Green, A.E.; Naghdi, P.M. On Undamped Heat Waves In An Elastic Solid. *J. Therm. Stress.* **1992**, *15*, 253–264. [[CrossRef](#)]
9. Green, A.E.; Naghdi, P.M. Thermoelasticity without Energy Dissipation. *J. Elast.* **1993**, *31*, 189–208. [[CrossRef](#)]
10. Povstenko, Y.Z. Fractional Heat Conduction Equation And Associated Thermal Stress. *J. Therm. Stress.* **2004**, *28*, 83–102. [[CrossRef](#)]
11. Dreher, M.; Quintanilla, R.; Racke, R. Ill-Posed Problems in Thermomechanics. *Appl. Math. Lett.* **2009**, *22*, 1374–1379. [[CrossRef](#)]

12. Lasiecka, I.; Wang, X. Moore-Gibson-Thompson Equation with Memory, Part II: General Decay of Energy. *Anal. PDEs* **2015**, *259*, 7610–7635. [[CrossRef](#)]
13. Quintanilla, R. Moore-Gibson-Thompson Thermoelasticity. *Math. Mech. Solids* **2019**, *24*, 4020–4031. [[CrossRef](#)]
14. Quintanilla, R. Moore-Gibson-Thompson Thermoelasticity with Two Temperatures. *Appl. Eng. Sci.* **2020**, *1*, 100006. [[CrossRef](#)]
15. Wang, J.-L.; Li, H.-F. Surpassing the Fractional Derivative: Concept of the Memory-Dependent Derivative. *Comput. Math. Appl.* **2011**, *62*, 1562–1567. [[CrossRef](#)]
16. Ezzat, M.A.; El-Karamany, A.S.; El-Bary, A.A. Generalized Thermo-Viscoelasticity with Memory-Dependent Derivatives. *Int. J. Mech. Sci.* **2014**, *89*, 470–475. [[CrossRef](#)]
17. Ezzat, M.A.; El-Karamany, A.S.; El-Bary, A.A. Generalized Thermoelasticity with Memory-Dependent Derivatives Involving Two Temperatures. *Mech. Adv. Mater. Struct.* **2016**, *23*, 545–553. [[CrossRef](#)]
18. Ezzat, M.A.; El-Karamany, A.S.; El-Bary, A.A. A Novel Magneto-Thermoelasticity Theory with Memory-Dependent Derivative. *J. Electromagn. Waves Appl.* **2015**, *29*, 1018–1031. [[CrossRef](#)]
19. Marin, M. The Lagrange Identity Method in Thermoelasticity of Bodies with Microstructure. *Int. J. Eng. Sci.* **1994**, *32*, 1229–1240. [[CrossRef](#)]
20. Marin, M. On Existence and Uniqueness in Thermoelasticity of Micropolar Bodies. *Comptes Rendus Acad. Sci. Paris Ser. II* **1995**, *321*, 475–480.
21. Abbas, I.A.; Marin, M. Analytical Solution of Thermoelastic Interaction in a Half-Space by Pulsed Laser Heating. *Phys. E Low-Dimens. Syst. Nanostructures* **2017**, *87*, 254–260. [[CrossRef](#)]
22. Kaur, I.; Lata, P.; Singh, K. Effect of Memory Dependent Derivative on Forced Transverse Vibrations in Transversely Isotropic Thermoelastic Cantilever Nano-Beam with Two Temperature. *Appl. Math. Model.* **2020**, *88*, 83–105. [[CrossRef](#)]
23. Kaur, I.; Lata, P. Rayleigh Wave Propagation in Transversely Isotropic Magneto-Thermoelastic Medium with Three-Phase-Lag Heat Transfer and Diffusion. *Int. J. Mech. Mater. Eng.* **2019**, *14*, 12. [[CrossRef](#)]
24. Van Do, T.; Hong Doan, D.; Chi Tho, N.; Dinh Duc, N. Thermal Buckling Analysis of Cracked Functionally Graded Plates. *Int. J. Struct. Stab. Dyn.* **2022**, *22*, 2250089. [[CrossRef](#)]
25. Doan, D.H.; Zenkour, A.M.; Van Thom, D. Finite Element Modeling of Free Vibration of Cracked Nanoplates with Flexoelectric Effects. *Eur. Phys. J. Plus* **2022**, *137*, 447. [[CrossRef](#)]
26. Craciun, E.M.; Baesu, E.; Soós, E. General Solution in Terms of Complex Potentials for Incremental Antiplane States in Prestressed and Pre-polarized Piezoelectric Crystals: Application to Mode III Fracture Propagation. *IMA J. Appl. Math. Inst. Math. Its Appl.* **2005**, *70*, 39–52. [[CrossRef](#)]
27. Lata, P.; Kaur, I.; Singh, K. Deformation in Transversely Isotropic Thermoelastic Thin Circular Plate Due to Multi-Dual-Phase-Lag Heat Transfer and Time-Harmonic Sources. *Arab J. Basic Appl. Sci.* **2020**, *27*, 259–269. [[CrossRef](#)]
28. Jafari, M.; Chaleshtari, M.H.B.; Abdolalian, H.; Craciun, E.-M.; Feo, L. Determination of Forces and Moments Per Unit Length in Symmetric Exponential FG Plates with a Quasi-Triangular Hole. *Symmetry* **2020**, *12*, 834. [[CrossRef](#)]
29. Craciun, E.M.; Carabineanu, A.; Peride, N. Antiplane Interface Crack in a Pre-Stressed Fiber-Reinforced Elastic Composite. *Comput. Mater. Sci.* **2008**, *43*, 184–189. [[CrossRef](#)]
30. Malik, S.; Gupta, D.; Kumar, K.; Sharma, R.K.; Jain, P. Reflection and Transmission of Plane Waves in Nonlocal Generalized Thermoelastic Solid with Diffusion. *Mech. Solids* **2023**, *58*, 161–188. [[CrossRef](#)]
31. Sharma, K.; Marin, M. Reflection and Transmission of Waves from Imperfect Boundary between Two Heat Conducting Micropolar Thermoelastic Solids. *Analele Univ. "Ovidius" Constanta-Ser. Mat.* **2014**, *22*, 151–176. [[CrossRef](#)]
32. Youssef, H.M.; El-Bary, A.A. Theory of Hyperbolic Two-Temperature Generalized Thermoelasticity. *Mater. Phys. Mech.* **2018**, *40*, 158–171. [[CrossRef](#)]
33. Lata, P.; Kaur, I. Thermomechanical Interactions in a Transversely Isotropic Magneto Thermoelastic Solids with Two Temperatures and Rotation Due to Time Harmonic Sources. *Coupled Syst. Mech.* **2019**, *8*, 219–245. [[CrossRef](#)]
34. Youssef, H.M.; El-Bary, A.A.; Elsibai, K.A. Vibration of Gold Nano Beam in Context of Two-Temperature Generalized Thermoelasticity Subjected to Laser Pulse. *Lat. Am. J. Solids Struct.* **2015**, *12*, 37–59. [[CrossRef](#)]
35. Rao, S.S. *Vibration of Continuous Systems*; John Wiley & Sons: Hoboken, NJ, USA, 2007; ISBN 0471771716.
36. Sharma, J.N.; Kaur, R. Transverse Vibrations in Thermoelastic-Diffusive Thin Micro-Beam Resonators. *J. Therm. Stress.* **2014**, *37*, 1265–1285. [[CrossRef](#)]
37. Lifshitz, R.; Roukes, M.L. Thermoelastic Damping in Micro- and Nanomechanical Systems. *Phys. Rev. B* **2000**, *61*, 5600–5609. [[CrossRef](#)]
38. Abbas, I.A. Free Vibrations of Nanoscale Beam Under Two-Temperature Green and Naghdi Model. *Int. J. Acoust. Vib.* **2018**, *23*, 289–293. [[CrossRef](#)]
39. Dhaliwal, R.S.; Singh, A. *Dynamic Coupled Thermoelasticity*; Hindustan Publication Corporation: New Delhi, India, 1980.
40. Mahdy, A.M.S.; Lotfy, K.; Ahmed, M.H.; El-Bary, A.; Ismail, E.A. Electromagnetic Hall Current Effect and Fractional Heat Order for Microtemperature Photo-Excited Semiconductor Medium with Laser Pulses. *Results Phys.* **2020**, *17*, 103161. [[CrossRef](#)]

Disclaimer/Publisher's Note: The statements, opinions and data contained in all publications are solely those of the individual author(s) and contributor(s) and not of MDPI and/or the editor(s). MDPI and/or the editor(s) disclaim responsibility for any injury to people or property resulting from any ideas, methods, instructions or products referred to in the content.